Am J Transl Res 2022;14(10):7012-7026
www.ajtr.org /ISSN:1943-8141/AJTR0143089

Original Article

Exosomes loaded with miR-665 inhibit the progression of osteosarcoma *in vivo* and *in vitro*

Bo Zhang[1*], Yang Yang[2*], Ran Tao[1], Chen Yao[1], Zhenyu Zhou[1], Yafeng Zhang[1]

Departments of [1]Orthopaedics, [2]Trauma Center, Affiliated Hospital of Nantong University, Nantong 226001, Jiangsu, China. [*]Equal contributors and co-first authors.

Received March 24, 2022; Accepted August 31, 2022; Epub October 15, 2022; Published October 30, 2022

Abstract: Objective: Osteosarcoma (OS) is the most common primary malignant bone tumor and has a poor prognosis. Recent research has suggested that miR-665 affects the progression of OS. Moreover, an exosome delivery system presents better targeting effects, higher permeability, and lower immunogenicity than other nano-delivery systems do. The purpose of this study is to explore whether an exosome loaded with the miR-665 delivery system can inhibit OS development. Methods: The miR-665 expression was detected through a quantitative real-time polymerase chain reaction assay. Transmission electron microscopy, nano-particle size analysis, and fluorescence microscope were utilized to observe exosomes. Cell growth was estimated by cell counting kit 8 and ethynyl deoxyuridine analyses. Assays of flow cytometry and Terminal-deoxynucleotidyl Transferase Mediated Nick End Labeling were introduced to test apoptosis *in vitro* or *in vivo*, respectively. Cell migration and invasion were measured using scratch and transwell assays. Engineered exosomes were prepared using electroporation. H&E staining was employed to observe necrotic cells and the function of heart, liver, spleen, lung and kidney. The expression of proteins was estimated by immunoblot analysis. Results: This work documented that the expression of miR-665 was downregulated in OS tissues. Additionally, we proved that the over-expression of miR-665 inhibited OS proliferation. Besides, we found that exosomes loaded with miR-665 had similar tumor-inhibiting effects *in vivo* and *in vitro*. Furthermore, we verified that the exosome delivery system exhibited good safety and target efficiency. Conclusion: This work proved that exosomes loaded with miR-665 inhibited the progression of OS *in vivo* and *in vitro* in a safe manner.

Keywords: Osteosarcoma, exosomes, miR-665

Introduction

Osteosarcoma (OS), the most frequent bone malignancy, features spindled stromal cells that are capable of producing osteoid tissue [1]. Most cases of OS are characterized by a bimodal age distribution, with the majority of cases occurring in adolescents aged 10-14 years, followed by those aged over 60 years [2]. Some patients with osteosarcoma experience tumor recurrence and distant metastasis after comprehensive treatment [3], which significantly reduced the survival rate of patients [4]. Currently, the commonly used clinical treatment of OS is mainly surgery combined with radiotherapy and chemotherapy. However, the therapeutic efficacy is limited by the disadvantages of low water solubility, fast clearance rate, poor targeting, high toxicity, and drug resistance [5]. Many studies have focused on improving the prognosis of OS by developing new treatment methods. It is still urgent to understand the pathogenesis of OS and gene-targeted therapy drugs.

MicroRNAs (miRNAs), the conserved non-coding small RNA, exist widely in organisms and affect gene expression at the post-transcriptional level [6]. MiRNAs are associated with important biological activities such as cell apoptosis, proliferation, differentiation, and development [7, 8]. A large number of studies have revealed that many specific miRNAs are closely related to OS development, such as miR-519d-3p, miR-671-5p, miR-22-3p and miR-877-3p, suggesting that miRNAs can serve as a biomarker for OS [9-12]. MiR-665 is a miRNA encoded by the nucleotide sequence on chromosome 14q32.2 in humans. Much evidence indicates that miR-665 plays a crucial role in

multiple malignant tumors. For example, miR-665 is significantly upregulated in breast cancer and promotes breast cancer progression by binding to the target gene NR4A3 [13]. In retinoblastoma, miR-665 down-regulates the expression of HMGB1, leading to the inactivation of the Wnt/β-catenin pathway, thereby inhibiting the development of retinoblastoma [14]. Dong et al. revealed that low expressed miR-665 is associated with poor prognosis of patients diagnosed with osteosarcoma [42]. Nevertheless, the molecular regulatory mechanism of miR-665 in OS is still unclear.

Exosomes, particles of 30-100 nm in diameter [15], regulate the formation of the immunosuppressive tumor microenvironment [16]. Studies have shown that exosomes carry mRNA, microRNA (miRNA), and long non-coding RNA (LncRNA) and regulate the biologic behavior of target cells by delivering these RNAs to target cells [17, 18]. MiRNAs secreted by exosomes have been proven to have a variety of biological functions in malignancies. For example, the metastasis of hepatocellular cancer is promoted by exosomes loaded with miR-21 [19, 20]. Exosomes carrying miR-29a secreted by non-small cell lung cancer bind toll-like receptors of the nearby macrophages to exert its pro-inflammatory response [21]. Compared to other nano-delivery systems such as lipids, polymers, and gold, live cell-derived exosomes have low immunogenicity, are highly biocompatible nanocarriers, and exhibit greater flexibility and very low cytotoxicity in loading the required antigens for efficient delivery [22, 23]. In addition, exosomes do not have the problem of adsorbed proteins to produce protein crowns, so they can achieve stable drug transport in the blood.

In this study, we used a variety of molecular biological approaches to verify that exosomes loaded with miR-665 derived from OS cells exhibit strong anti-tumor properties *in vivo* and *in vitro*, which provides an important treatment strategy for OS.

Material and methods

Clinical samples

Thirty-two patients (age, 18-70) with OS who were hospitalized in the Orthopaedics Department of Affiliated Hospital of Nantong University and underwent surgical treatment from July 2020 to July 2021 were selected for this study. None of the patients received adjuvant therapy such as radiotherapy and chemotherapy before surgery. Pathologic types were based on *WHO Osteosarcoma Classification Criteria*. Para-cancer tissue from each osteosarcoma patient served as a control. All experiments abided by the ethical guidelines of the *Helsinki Declaration* and were approved by the Ethics Committee of Affiliated Hospital of Nantong University (No. S20211014-001). All the patients signed informed consent forms.

RNA extraction and quantitative real-time PCR

Total RNA was extracted according to the kit's protocol (A2010A0402, BioTNT, China). Complementary DNAs (cDNAs) were obtained by a reverse transcription kit (A2010S0406, BioTNT, China) following the instructions, and the level of miR-665 was estimated with a Target Gene Detection kit (A2010S0414, BioTNT, China) according to the manufacturer's protocol. The primers are listed as follows: miR-665, forward: 5'-GGTGAACCAGGA GGCTGAGG-3' and reverse: 5'-CAGTGCAGGGTCCGAGGTAT-3'. U6, forward: 5'-CTCGCTTCGGCAGCACA-3' and reverse: 5'-AACGCTTCACGAATTTGCGT-3'.

Cell counting kit-8 (CCK-8) assay

MG63 cells (10,000 cells/well) were cultured in 96-well plates. At 24 h, 48 h, and 72 h, 10 μL of CCK-8 solution was supplemented to each well and incubated with MG63 cells at 37°C for another 3 h. Then the absorbance was tested at the wavelength of 450 nm to assess the cell viability.

Flow cytometric analysis of cell apoptosis

The cells were seeded into 6-well plates and treated with indicated vectors for 24 h. Then the cells were collected and washed utilizing cold PBS. Next, the cell suspension was incubated with PI and Annexin V-EGFP according to the kit procedures (KeyGen Biotech Co., Ltd., Nanjing, China). Finally, the apoptotic cells were recorded by employing an FACS assay.

Immunoblot

MG63 cells or OS tissues were lysed with RIPA buffer (AKR-191, BioTNT, China), and protein concentrations were examined with a BCA pro-

Table 1. Antibody information

Antibodies	Dilution rates	Product codes	Manufacturers
β-actin	1:1000	PA5-35201	Invitrogen
CD63	1:1000	Ab134045	Abcam
TSG101	1:1000	Ab125011	Abcam
BAX	1:2000	PA5-17216	Invitrogen
Bcl-2	1:10000	AM4302	Invitrogen
Cleaved-Caspase-3	1:1000	ab155938	Abcam
Cleaved-Caspase-9	1:1000	ab2324	Abcam
PCNA	1:500	ab92552	Abcam
Goat Anti-mouse IgG H&L (HRP)	1:10000	ab6728	Abcam
Goat Anti-rabbit IgG H&L (HRP)	1:10000	ab6721	Abcam

tein assay kit (23227, Thermo Scientific). The 30 μg proteins were separated employing 12.5% SDS-PAGE and transferred onto 0.45 μm PVDF membranes (millipore-IPVH00010, BioTNT, China). Then the membranes were blocked using 5% bovine serum albumin for another 1 h and incubated with primary antibodies (**Table 1**) at 4°C overnight. Next, the membranes were incubated with specific secondary antibodies for 1 h. Eventually, the protein bands were visualized with an Enhanced ECL Chemiluminescence Detection Kit (E411-04, Vazyme, China) and a ChemiDoc XRS imaging system.

Cell exosomes collection

The culture solution containing about 1 * 10^7 cells was collected into a 50 mL centrifuge tube and centrifuged at 800 g for 5 minutes to collect the supernatant medium, which was further centrifuged at 2,000 × g for 10 min at 4°C. The centrifuged supernatant medium was collected and then filtered using a 0.22 μm microporous membrane. Then, the mixture was centrifuged at 100,000 g, 4°C for 2 hours. After centrifugation, the supernatant was discarded and resuspended with PBS. Next, the solution was centrifuged for 2 h at 100,000 g at 4°C, followed by discarding the supernatant and resuspending the exosomal pellet in 100 μL PBS for subsequent experiments or storing at 80°C.

Engineered exosomes containing miR-665 were prepared by electroporation

The concentration of exosomes was detected by BCA Protein Quantification Kit following its instructions. Next, exosomes with a total protein concentration of 10 μg/mL and 400 nM miR-665 were mixed in 400 μL PBS, and then added into an electric cup. Two groups of electroporation parameters were set (400 V, 2.5 ms/15 ms). After the electric shock, the samples were placed on ice, marked as required, sent for inspection after ultra-high-speed centrifugation, and separated at -80°C for storage for subsequent tests. The loading rate was measured by Apogee ultrasensitive flow cytometry. miR-(/FAM/CY3) was used in this experiment.

Exosome labeling

The exosome was labeled by employing the PKH26 Cell Linker Kit (MX4021, Shanghai Maokang Biotechnology Co., Ltd., Shanghai, China) following the instructions. Briefly, the PKH26 fluorescent dye was diluted to 2 × 10^6 M and was incubated with exosomes at room temperature for 20 min, followed by stopping the reaction with 5% bovine serum albumin (37520, Thermo Scientific, USA). Then exosome was re-suspended, centrifugated and extracted in PBS. The cell nuclei were stained with 4',6-diamidino-2-phenylindole (DAPI, 28718-90-3, Glpbio, USA) according to the manufacturer's protocol. After that, labeled exosomes were taken up by OS cells and were observed utilizing a confocal laser scanning microscope (FV3000, Olympus, Japan).

Transwell invasion and migration experiment

The cells to be measured were cultured to a logarithmic growth stage, then were digested and washed with PBS and a serum-free medium one time successively, and then suspended with serum-free medium. For the invasion

experiment, Matrigel gel (BD company, 356234) was taken from -20°C and put in the refrigerator overnight at 4°C. At 4°C, Matrigel gel was diluted with serum-free cell medium to 300 μL/mL. Next, 100 μL Matrigel Gel solution was applied evenly on the upper surface of the PET membrane which was then placed into a 24-well plate. The plate was placed at 37°C for 3 h and was taken out and dried overnight on a super clean workbench. This step was skipped if the migration experiment was performed. Then 600-800 μL medium containing 10% serum was supplemented in the lower chamber (i.e., the bottom of the 24-well plate). The 100-150 μL cells suspended in 600 μL serum-free medium were added to the upper chamber, and were continued to culture in the incubator for 24 h. The lower surface of the PET membrane was soaked in 70% methanol solution, fixed for 30-60 min, stained with crystal violet and examined under a microscope. The number of cells on the lower surface of the PET membrane was calculated, and 5 fields in the middle and around the plate were calculated, and the average value was taken.

Scratch test

5×10^5 cells were seeded in 6-well plates and 200 μL sterile tips were used to evenly draw a horizontal line in the bottom of the plate. The exfoliated cells were washed using PBS 3 times. Then the plates were put into a 37°C 5% CO_2 incubator for cultivation. The width of the scratch was measured and recorded at 0, 6, 12 and 24 hours.

Immunohistochemical (IHC) analysis

Tissues were embedded in paraffin, cut into slices and deparaffinized. Next, the slices were incubated with citrate buffer (pH=6) and immersed in 3% H_2O_2. Then the slices were blocked for 30 min utilizing 10% goat serum, followed by incubating with rabbit PCNA antibodies (**Table 1**) at 4°C overnight. Finally, the pictures were captured under high-power magnification (200 ×) by utilizing a microscope (CX31-LV320, Olympus, Japan).

Hematoxylin & eosin (H&E) staining

After removing fat and connective tissue, the tissue samples were fixed using 4% paraformaldehyde (P1110, BioTNT, China). Then, the tissues were dehydrated at 4°C for 24-48 h and embedded in paraffin. Next, the samples were cut into 4 μm slices and stained by employing Hematoxylin and Eosin Staining Kit (C0105M, Beyotime, China). Finally, a microscope (CX31-LV320, Olympus, Japan) was introduced to observe the pathological changes.

TUNEL assay

Tissues were embedded in paraffin, cut into slices and deparaffinized. Then the slices were incubated with protease K (P9460, BioTNT, China) for 15 min. Next, the apoptosis rate of tissues was tested using an Apo-Brdu-Ihct DNA Breakage Detection Kit (BioTNT, China) according to its instruction. Finally, a microscope (CX31-LV320, Olympus, Japan) was introduced to observe and analyze the slices.

Xenograft mouse model and in vivo imaging

The 4-week-old nude mice obtained from Guangdong Medical Laboratory Animal Center (Guangzhou, China) were divided into 4 groups randomly (n=8 mice/group): Ad-NC mimic group, Ad-miR-665 mimic group, unloaded Exo group and miR-665 Exo group. Then MG63 cells (1×10^7) stably expressing Ad-NC mimic orAd-miR-665 mimic were injected into the armpits of mice in Ad-NC mimic or Ad-miR-665 mimic group, respectively. Mice in the unloaded Exo or miR-665 Exo group were injected with MG63 cells (1×10^7), followed by injecting with 60 μg unloaded Exo or miR-665 Exo intravenously every 2 days for five weeks. After 6 days, the volume of tumors was measured every day ($0.5 \times \text{length} \times \text{width}^2$) and the exosomes labeled with PHK26 were observed using an IVIS-200 Imaging System (Xenogen Corporation, USA). Five weeks later, the mice were sacrificed, and xenografts were assessed and weighed. All protocols related to nude mice were supported by the ethical guidelines of the Helsinki Declaration and were approved by the Animal Ethics Committee of Affiliated Hospital of Nantong University.

Integrated analysis of osteosarcoma data

The miRNA expression data of OS tissues from the miRcancer database (http://mircancer.ecu.edu/), Genecards database (https://www.genecards.org/) and GSE70415 dataset from the GEO database (https://www.ncbi.nlm.nih.gov/

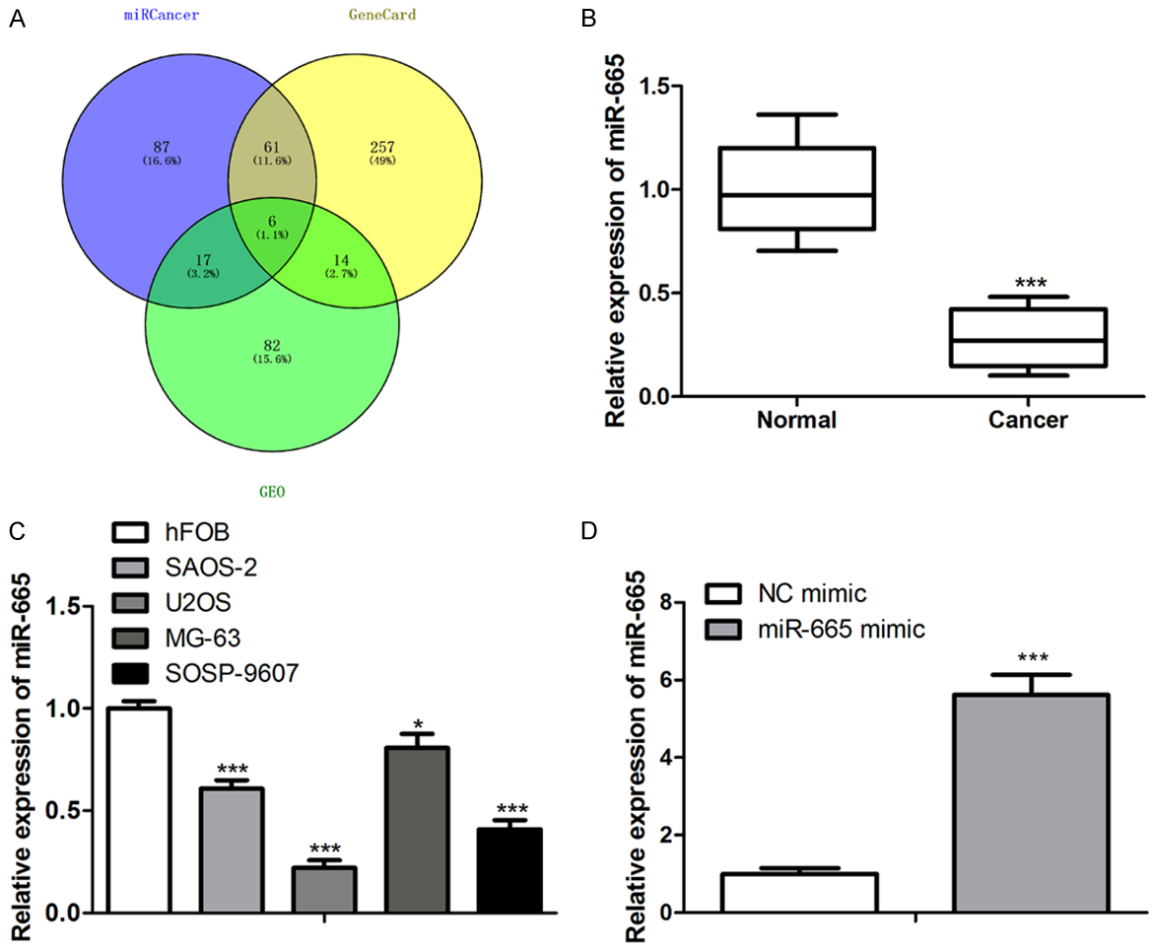

Figure 1. MiR-665 expression was down-regulated in the OS tissues and cell lines. A: Integrated OS data from miRCancer, GEO and Genecards database and found 6 OS-associated overlapping microRNAs; B: Q-PCR results showed that the expression of miR-665 was significantly down-regulated in the OS tissues compared to the normal tissues. ***P<0.001 vs. Normal; C: Q-PCR results revealed that the expression level of miR-665 in these osteosarcoma cell lines was significantly lower than that in normal osteoblasts. *P<0.05, ***P<0.001 vs. hFOB; D: Q-PCR results indicated that miR-665 was successfully overexpressed in osteosarcoma cell lines. ***P<0.001 vs. NC mimic.

geo/) are powerful data to study miRNAs correlated with osteosarcoma. These collected data were normalized by the limma package in R (4.0.5 version), and the Venn diagram was drawn by the VennDiagram package in R (4.0.5 version) [24, 25].

Statistical analysis

All the experiments were carried out at least three times independently. Data were analyzed utilizing SPSS (version 24, SPSS (IBM) Inc., Illinois, USA) and presented as mean ± standard deviation (SD). Unpaired student's t-tests or one-way ANOVA followed by Tukey's test were used for data comparison (SPSS 12.0). Statistical significance was determined as $P<0.05$.

Results

MiR-665 expression was down-regulated in the OS tissues and cell lines

To investigate the differential expression of miR-665 in OS and normal tissues, we integrated data related to OS in the miRCancer, GEO, and Genecards database and found 6 OS-associated overlapping miRNAs (**Figure 1A**). We used qPCR to detect the miR-665 expression in clinical tissues. As exhibited in **Figure 1B**, miR-665 was significantly down-regulated in the OS tissues compared to the normal tissues (**Figure 1B**). We further detected the expression of miR-665 in several osteosarcoma cell lines and normal osteoblasts by qPCR. The results showed that the expression

level of miR-665 in these osteosarcoma cell lines was significantly lower than that of normal osteoblasts (**Figure 1C**). To investigate the effect of miR-665 on osteosarcoma development, we successfully overexpressed miR-665 in osteosarcoma cell lines (**Figure 1D**).

Exosomes loaded with miR-665 showed the common characteristics of general exosomes

To detect whether the exosomes loaded with miR-665 have the general characteristics of exosomes, transmission electron microscopy (TEM) was done. Results showed that the exosomes loaded with miR-665 expressed a higher level of miR-665 and were in the shape of saucers with a diameter of about 100 nm, which was the same as the unloaded exosomes (**Figure 2A**, **2B**). The results of nano-particle size analysis showed that the particle sizes of exosomes derived from osteosarcoma cells were concentrated in the range of 80-100 nm, which was consistent with the consensus of exosomal diameter of 30-150 nm (**Figure 2C**). Immunoblot was used to identify exosome molecular markers, and the results showed that exosomes derived from osteosarcoma cells specifically expressed CD63 and TSG101, while the culture medium after exosome extraction did not express such molecules (**Figure 2D**). Moreover, PKH26 labeled exosomes were injected into experimental mice by tail vein injection, and then red fluorescent substances at the osteosarcoma site were observed under a fluorescence microscope as exosomes (**Figure 2E**).

Exosomes loaded with miR-665 exhibited proliferation-inhibition and apoptosis-induction effects on OS cells

Next, we tested whether the miR-665 mimic and exosomes loaded with miR-665 exerted tumor-inhibition effects on OS cell lines. qRT-PCR assay illustrated that miR-665 mimic and miR-665 Exo exhibited loading efficiency of miR-665 (**Figure 3A**). CCK-8 analysis suggested that the miR-665 mimic and exosomes loaded with miR-665 significantly reduced the cell viability of MG-63 cells (**Figure 3B**). Furthermore, the EdU assay illustrated that the proliferation ability of OS cells was notably reduced by the miR-665 mimic and exosomes loaded with miR-665 (**Figure 3C**). FACS assay analysis suggested that the miR-665 mimic and exosomes loaded with miR-665 induced more apoptotic cells in the MG-63 cell line (**Figure 3D**). Immunoblot analysis indicated that miR-665 overexpression up-regulated the content of the pro-apoptotic protein of Bax, and cleaved caspase-3 as well as cleaved caspase-9, but decreased levels of anti-apoptotic protein of Bcl-2 (**Figure 3E**). Collectively, these experimental results proved that exosomes loaded with miR-665 exhibited proliferation-inhibition and apoptosis-induction effects on OS cells.

Exosomes loaded with miR-665 inhibited the migration and invasion of OS cells

Scratch and transwell chamber assays showed that miR-665 mimic and exosomes loaded with miR-665 markedly inhibited migration and invasion of OS cells (**Figure 4A**, **4B**). At the molecular level, western blot assays revealed that miR-665 mimics decreased the protein levels of MMP-2 and MMP-9 in OS cells (**Figure 4C**). These results indicated that miR-665 inhibited the migration and invasion of OS cells.

Exosomes loaded with miR-665 exerted tumor-inhibition effects on OS in vivo

We then explored whether exosomes loaded with miR-655 had the same tumor-inhibition effects *in vivo*. MG63 cells were injected into nude mice. One week after the in-situ implantation of OS cells, NC mimic, miR-655 mimic, Unloaded-exo, and miR-655-exo were injected into the tumor-bearing mice through the tail vein. A bioluminescence imaging assay was performed on the mice after a five-week treatment to measure the volume of the transplanted tumor. The results showed that the miR-655 mimic and exosomes loaded with miR-655 significantly inhibited the growth of OS (**Figure 5A**). We also proved that both miR-655 mimic and exosomes loaded with miR-655 significantly reduced the tumor volume and weight (**Figure 5B**, **5C**). H&E staining indicated that the more necrotic cells were induced by miR-655 mimic and exosomes loaded with miR-655 than that in the control group (**Figure 5D**). IHC results showed that the miR-655 mimic and exosomes loaded with miR-655 significantly reduced the protein levels of PCNA (**Figure 5E**). TUNEL assay indicated that the miR-655 mimic and exosomes loaded with miR-655 induced more apoptotic cells (**Figure 5E**). The q-PCR results indicated that miR-655 was successfully over-

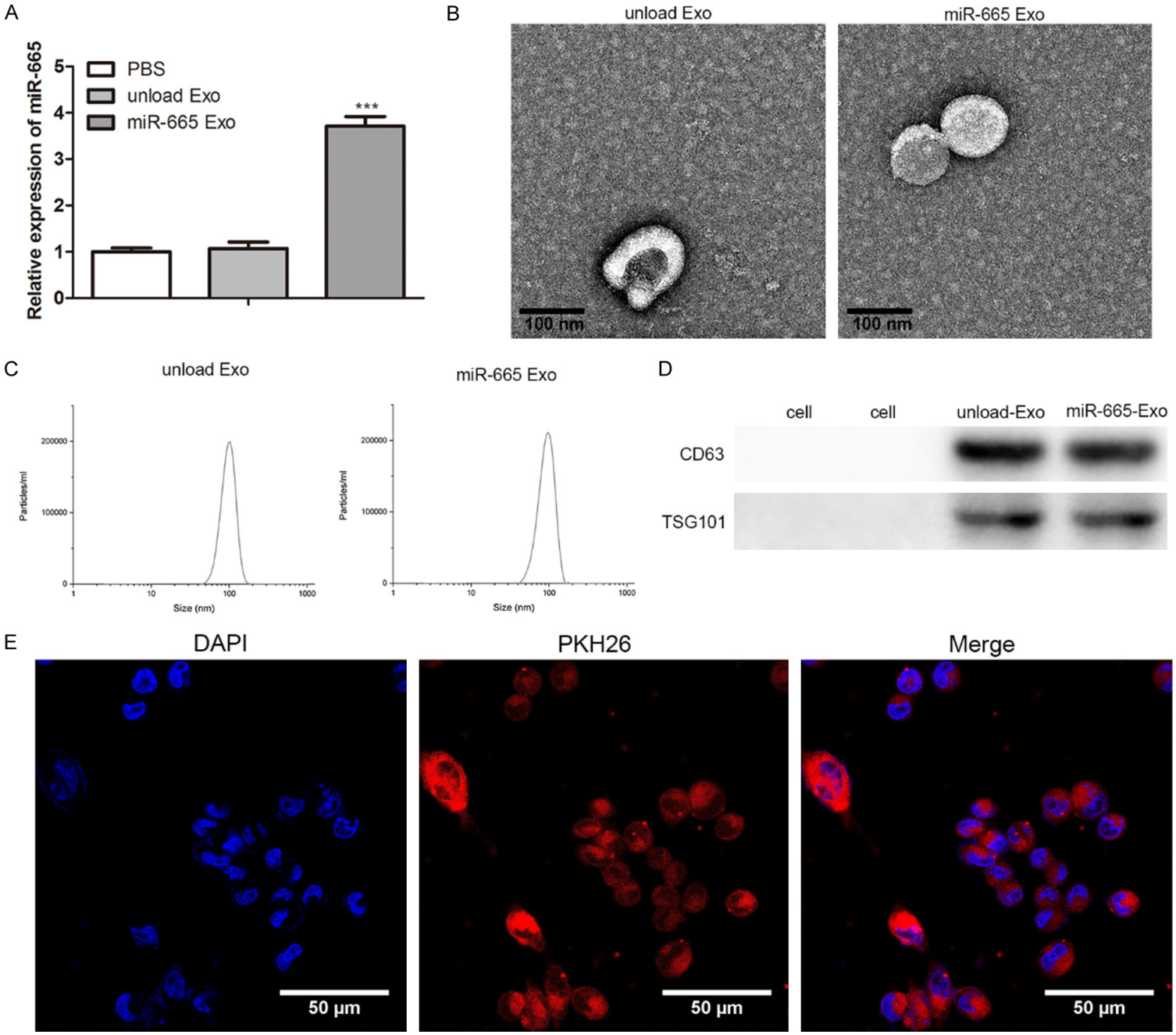
A
Relative expression of miR-665
PBS
unload Exo
miR-665 Exo
***
B
unload Exo
miR-665 Exo
100 nm
100 nm
C
unload Exo
miR-665 Exo
Particles/ml
Size (nm)
D
cell
cell
unload-Exo
miR-665-Exo
CD63
TSG101
E
DAPI
PKH26
Merge
50 μm
50 μm
50 μm

Figure 2. Tracing of exosomes derived from OS cells. A: q-PCR results showed that when exosomes loaded with miR-665 were extracted, the expression of miR-665 in exosomes increased significantly; B: Transmission electron microscopy (TEM) results showed that the negative-stained exosomes were in the shape of saucers with a diameter of about 100 nm; C: The results of nano-particle size analysis showed that the particle sizes peak of exosomes derived from pericytes were at about 100 nm; D: Immunoblot results showed that exosomes derived from OS cells specifically expressed CD63 and TSG101, while the culture medium after exosome extraction did not express such molecules; E: PKH26 labeled exosomes were injected into experimental mice by tail vein injection, and then the red fluorescent substances in the OS site were observed under a fluorescence microscope as exosomes; B: ***P<0.001 vs. PBS.

expressed *in vivo* (**Figure 5F**). The results above revealed that exosomes loaded with miR-665 exerted tumor-inhibiting effects on OS *in vivo*.

Safety of exosome treatment

We also evaluated the safety of exosome therapy. There was no obvious difference in body weight among the Unload-Exo, miR-655 mimic and miR-655-exo groups (**Figure 6A**). There were no significant differences in the liver function and blood routine tests of the three groups by a biochemical blood test (**Figure 6B**). The H&E staining of the heart, liver, spleen, lung, and kidney showed that there was no significant difference among the three groups (**Figure 6C**).

Discussion

Osteosarcoma is the most common type of primary bone malignancy in children and adolescents, with a poor prognosis and heterogeneous histological and molecular characteristics [26]. Previous studies have showed that the survival rate of patients with local osteosarcoma was about 65%, and that of patients with metastatic and recurrent osteosarcoma was only 20% [27]. Despite the rapid development of therapeutic methods, the clinical therapeutic effects on OS are still poor [28]. Therefore, we need to further explore the pathogenesis and progress of OS. The development of molecular biology research provides a basis for studying the pathogenesis of OS. Besides, the efficacy of chemotherapeutic drugs is limited by their poor solubility and high toxicity to normal tissues and organs. Exosomes with endogenous and double-layer fluid lipid vesicles have natural advantages incomparable to other artificial materials in terms of safety and fluid retention. In recent years, studies have found that abnormal miRNA expression and exosomes secreted from cancer cells play multiple roles in the occurrence and development of OS, including regulation of signaling pathways, epithelial-mesenchymal transformation and drug resistance [9, 29, 30].

In this study, we verified that miR-665 was down expressed in OS tissue samples and OS cell lines. Furthermore, we found that the miR-665 mimic and exosomes loaded with miR-665 have a tumor-inhibitory effect. In addition, we have verified that this exosome can play a similar tumor suppressor role *in vitro*. Importantly, exosomes loaded with miR-665 have good safety and targeting properties according to experiments. Based on the facts above, we proved that exosomes loaded with miR-665 derived from OS cells could inhibit the progression of OS.

Exosomes are bioactive nanoscale vesicles secreted by cells and are cup-shaped vesicles with a diameter of 40-140 nm and in lipid bilayer structure [31, 32]. For example, Cai et al. found that exosomes loaded with miR-9 produced by mesenchymal stem cells from bone marrow inhibited the occurrence and development of bladder cancer by down-regulating ESM1 [33]. It has been reported that most chemotherapeutic drugs for cancers have low solubility in blood, short half-life and poor utilization rate [34]. One of the current technologies used to deliver drugs to the tumor site efficiently and highly targeted to the tumor site is to encapsulate drugs in tumor-targeting vectors or nanocarriers, which often contain targeting factors that facilitate the entry into the tumor region. However, the artificial nature of nanocarrier systems leads to problems related to toxicity *in vivo* [34]. Exosomes, especially engineering exosomes, as extensive endogenous carriers, have many favorable characteristics of drug delivery: small size, immune escape, the long half-life, and subtypes that target tumor cells [35]. More importantly, exosomes can effectively load hydrophilic drugs and hydrophobic drugs. In this study, exosomes extracted from

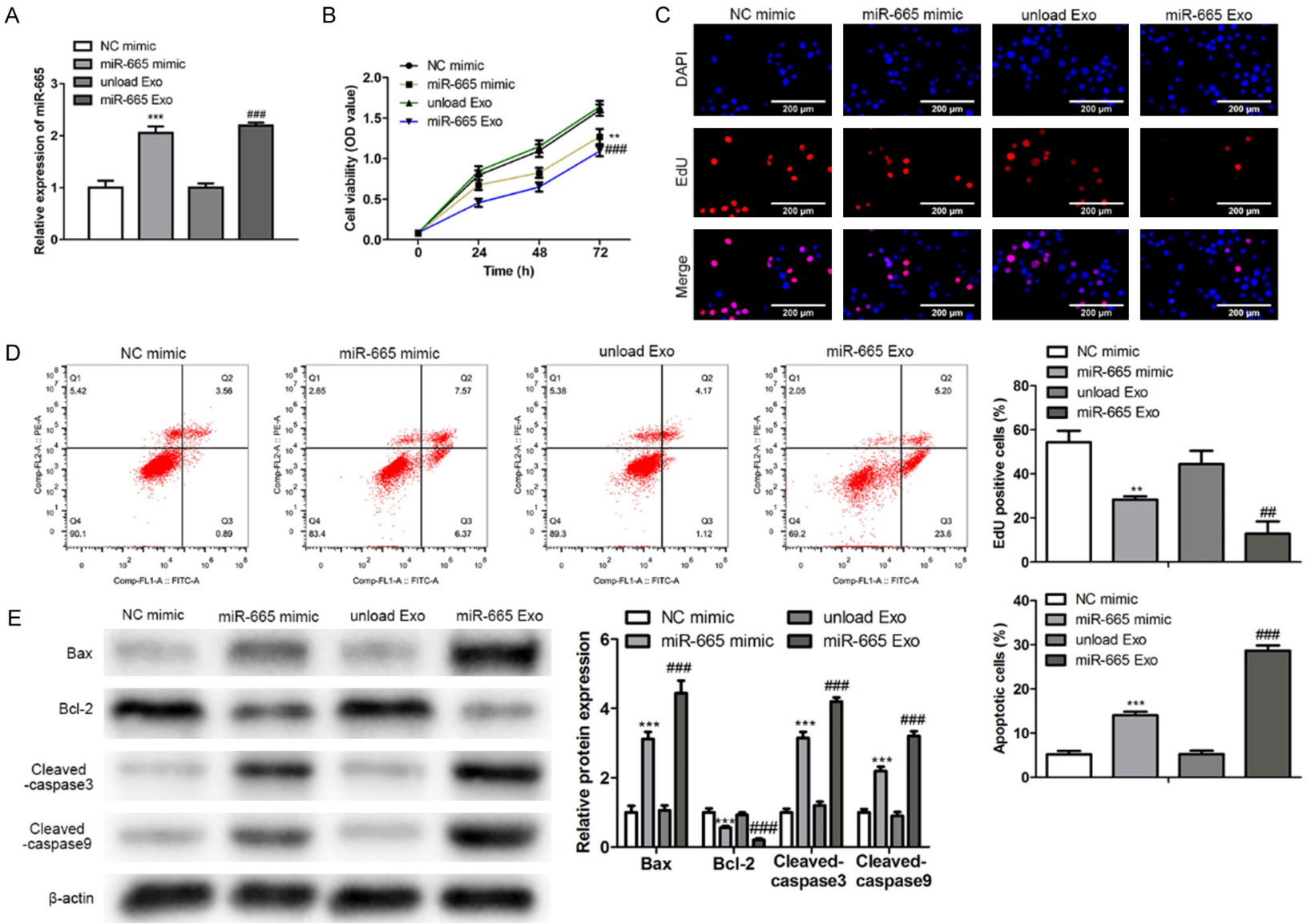

Figure 3. MiR-665 inhibited the proliferation of OS cells. A: Expression level of miR-665 in different groups. ***P<0.001 vs. NC mimic; ###P<0.001 vs. unload Exo; B: In the CCK-8 test, cell viability was measured by OD value after MG63 cells were transfected with NC mimic, miR-665 mimic, unloaded exosomes, or exosomes loaded with miR-665 for 24 h, 48 h, and 72 h. **P<0.01 vs. NC mimic; ###P<0.001 vs. unload Exo; C: EdU assay detection showed that miR-665 mimic and exosomes loaded

with miR-665 induced more apoptotic cells. **P<0.01 vs. NC mimic; ##P<0.01 vs. unload Exo; D: FACS for cell distribution analysis showed that miR-665 mimic and exosomes loaded with miR-665 induced more apoptotic cells. ***P<0.001 vs. NC mimic; ###P<0.001 vs. unloaded Exo; E: Immunoblot analysis showed that miR-665 mimic and exosomes loaded with miR-665 significantly increased the levels of the pro-apoptotic protein of Bax, cleaved caspase-3 and cleaved caspase-9, but decreased levels of anti-apoptotic protein of Bcl-2. ***P<0.001 vs. NC mimic; ###P<0.001 vs. unload Exo.

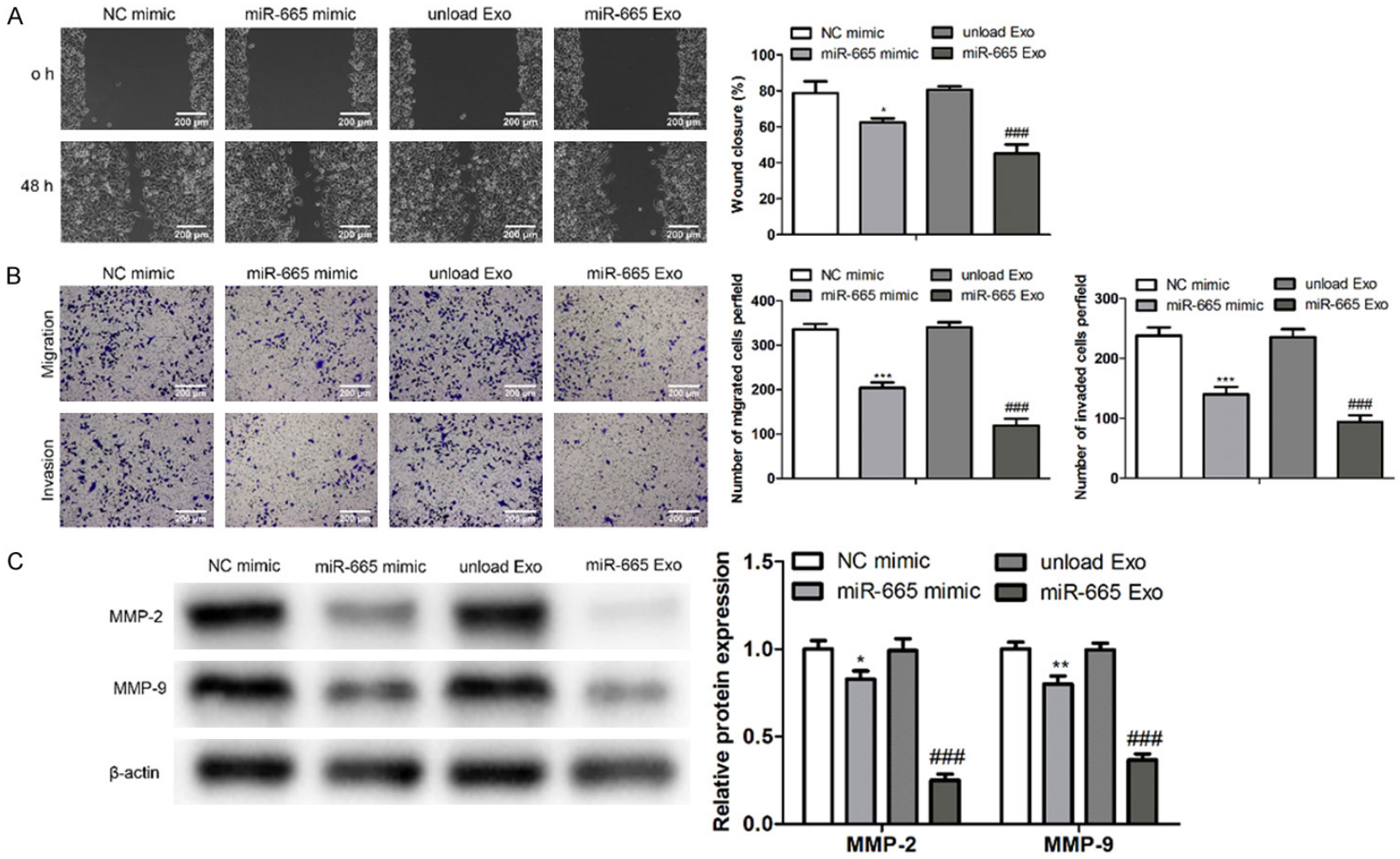

Figure 4. MiR-665 inhibited the migration and invasion of OS cells. Scratch (A) and transwell (B) chamber assays showed that the miR-665 mimic and exosomes loaded with miR-665 markedly inhibited migration and invasion of OS cells; (C) Western blot assays revealed that the protein levels of MMP-2 and MMP-9 were decreased by miR-665 in OS cells. *P<0.05, **P<0.01, ***P<0.001 vs. NC mimic; ###P<0.001 vs. unloaded Exo.

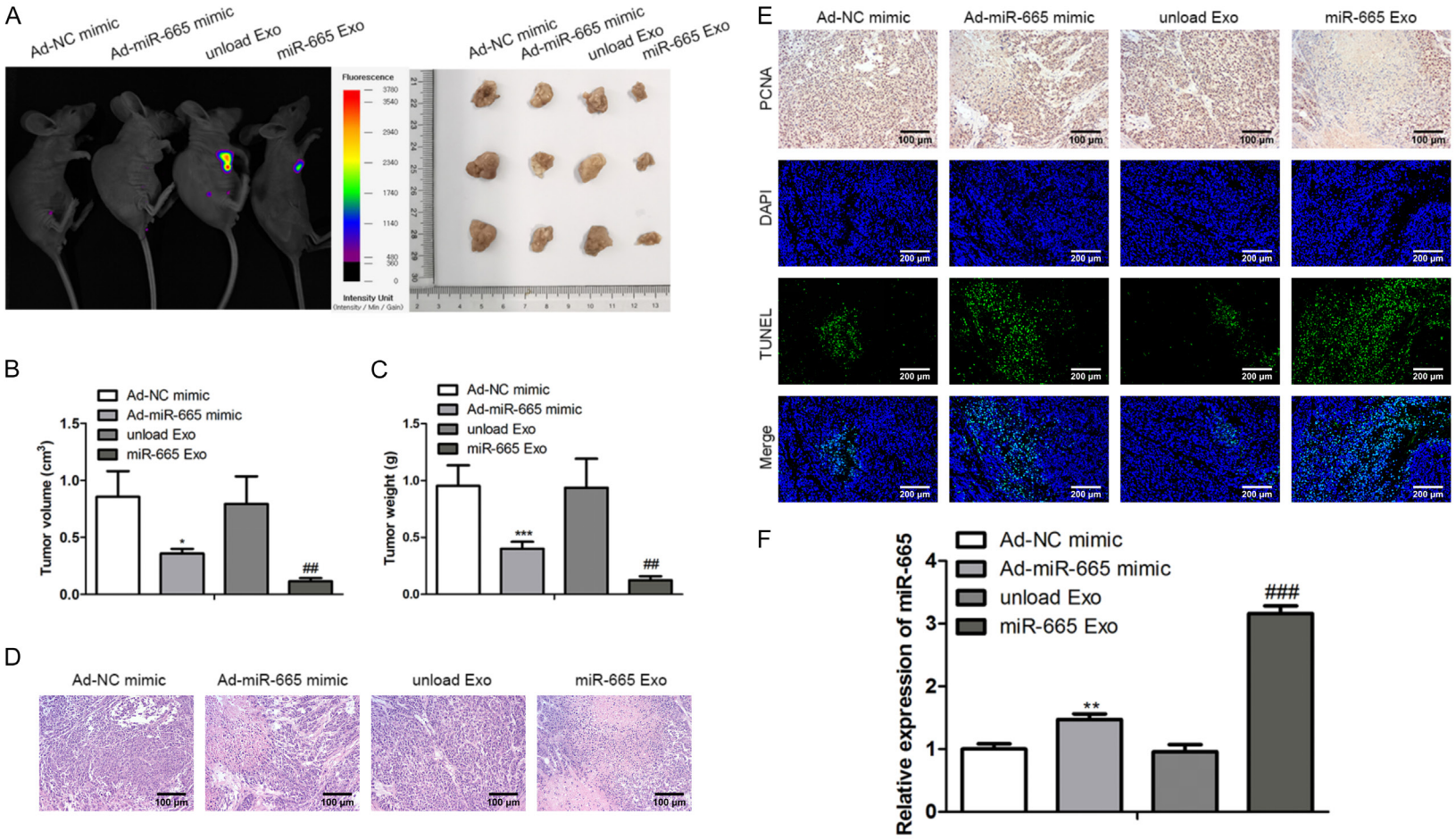

Figure 5. The exosomes loaded with miR-665 exerted tumor-inhibition effects on OS *in vivo*. A: *In vivo* bioluminescence imaging was performed on the treated mice after four-week treatment to measure the volume of the transplanted tumor. The results showed that the exosomes loaded with miR-665 significantly inhibited the growth of gliomas; B, C: Size and weight analysis of OS showed that exosomes loaded with miR-665 had strong tumor-inhibiting effects on OS; D: H&E staining indicated that the exosomes loaded with miR-665 group induced more necrotic cells than that in the unloaded-Exo group; E: TUNEL assay indicated that miR-665-Exo induced more apoptotic cells. IHC test showed that miR-665-Exo reduced the protein level of PCNA; F: q-PCR detection suggested that miR-665 expression levels in exosomes significantly increased. $^{*}P<0.05$, $^{**}P<0.01$, $^{***}P<0.001$ vs. Ad-NC mimic; $^{\#\#}P<0.01$, $^{\#\#\#}P<0.001$ vs. unloaded Exo.

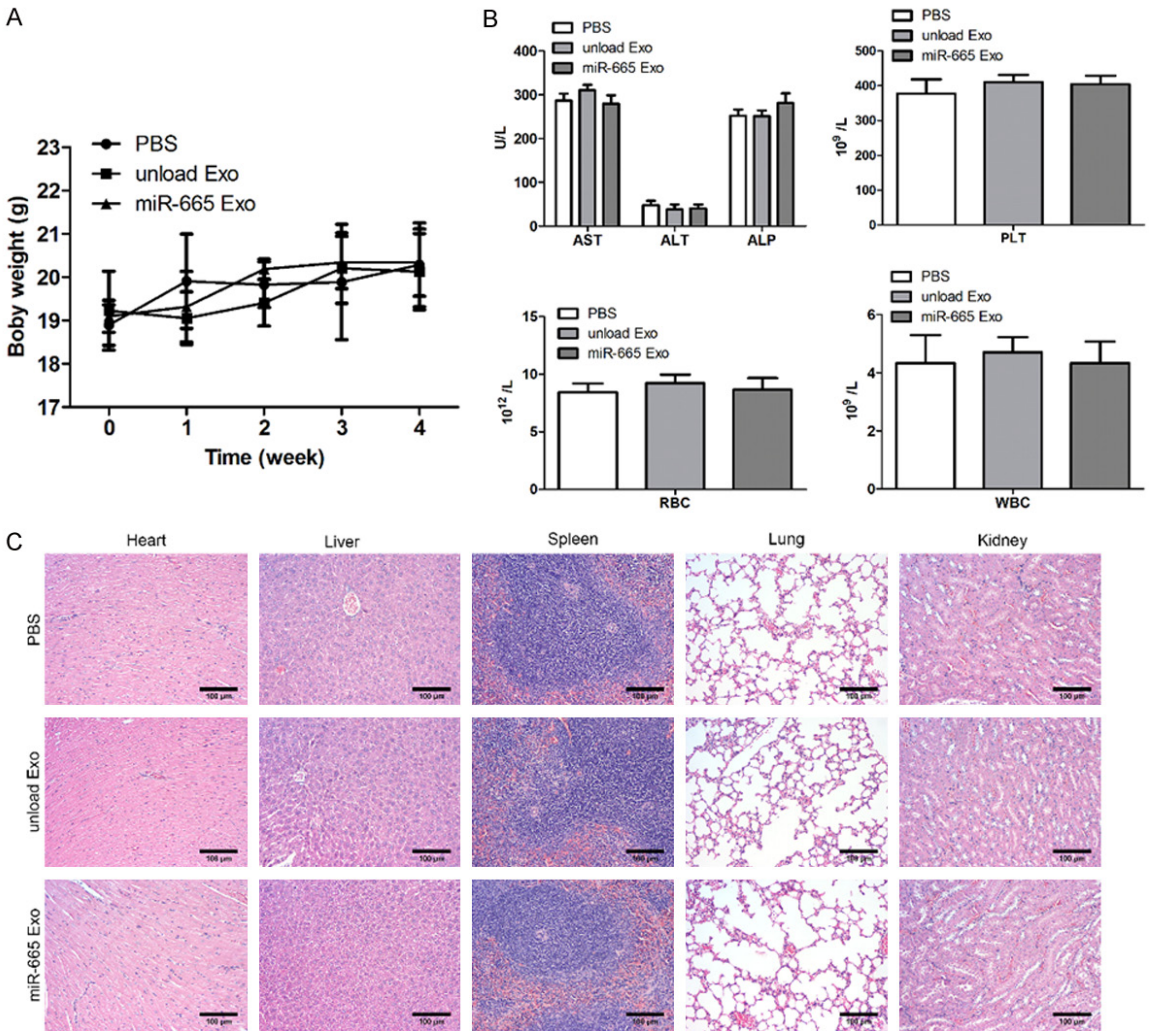

Figure 6. The evaluation of the safety of exosome treatment. A: Body weight detection showed that there was no significant difference between the unloaded-Exo and miR-665-Exo groups; B: Liver function of the mice in three groups by biochemical blood test showed that there were no significant differences; C: The functional tests of heart, liver, spleen, lung and kidney showed no significant difference among the three groups.

osteosarcoma cells were observed by TEM to be round or like a tea holder/cup structure, with dark surrounding color and a light center with an obvious three-dimensional shape. The diameter was about 100 nm, and the peak particle size was about 100 nm (**Figure 2B**, **2C**). The concentration of distribution was high at one time, which was consistent with the characteristics of exosomes reported in the previous studies (**Figure 2B**, **2C**) [36].

Raimondi et al. suggested that the role of osteosarcoma cell-derived exosomes play in bone metabolism is associated with some specific miRNAs and suggested that these exosomes are involved in osteoclast differentiation and bone resorption activity [37]. Osteosarcoma cell-derived exosomes loaded with miRNAs are involved in the progression of diverse cancers. For example, Gong et al. found that exosome miR-675 of osteosarcoma promoted the migration and invasion of hFOB osteoblasts by targeting CALN1 [38]. Shimbo et al. proposed that exosomes containing miR-143 secreted by mesenchymal stem cells inhibited the migration of osteosarcoma cells [39].

Moreover, studies have shown that miR-665 is expressed differently and plays crucial roles in different cancer tissues such as neuroblastoma, esophageal cancer, lung cancer, liver cancer, gynecological tumor, and prostate cancer

[14, 40, 41]. In addition, in osteosarcoma, the overexpressed miR-665 inhibits the proliferation, EMT, and invasion of osteosarcoma cells, and the expression of miR-665 is negatively correlated with the expression of the Rab23 gene [42]. However, the expression of exosomes secreted by OS cells loaded with miR-665 in OS and the related molecular regulatory mechanism remains unclear. In this article, we suggest that the exosomes loaded with miR-665 exerted tumor-inhibition effects on OS *in vitro* and *in vivo* (**Figures 3**-**5**). Furthermore, this investigation also revealed that exosomes loaded with miR-665 are safe (**Figure 6**).

There exist several limits in this study. For example, we only verified that exosomes loaded with miR-665 exert essential effects on the OS progression. However, more experiments will be conducted to reveal the detailed signaling pathway regulated by exosomes loaded with miR-665 in OS. Additionally, genes targeted by miR-665 in OS requires further exploration in subsequent studies.

In summary, exosomes loaded with miR-665 inhibit the progression of OS *in vivo* and *in vitro*. This may be used as a treatment strategy for OS.

Acknowledgements

This work was supported by the National Natural Science Foundation of China (81501913) and the Natural Science Fund of Jiangsu Province, China (BK20151275).

Disclosure of conflict of interest

None.

Address correspondence to: Drs. Bo Zhang and Yafeng Zhang, Department of Orthopaedics, Affiliated Hospital of Nantong University, No. 20 Xisi Road, Chongchuan District, Nantong 226001, Jiangsu, China. Tel: +86-0513-81161521; E-mail: zhangboshili@163.com (BZ); fcius2004@hotmail.com (YFZ)

References

[1] Briccoli A, Rocca M, Salone M, Guzzardella GA, Balladelli A and Bacci G. High grade osteosarcoma of the extremities metastatic to the lung: long-term results in 323 patients treated combining surgery and chemotherapy, 1985-2005. Surg Oncol 2010; 19: 193-199.

[2] Ottaviani G and Jaffe N. The epidemiology of osteosarcoma. Cancer Treat Res 2009; 152: 3-13.

[3] Mortus JR, Zhang Y and Hughes DP. Developmental pathways hijacked by osteosarcoma. Adv Exp Med Biol 2014; 804: 93-118.

[4] Powers M, Zhang W, Lopez-Terrada D, Czerniak BA and Lazar AJ. The molecular pathology of sarcomas. Cancer Biomark 2010; 9: 475-91.

[5] Gangi A, Chung A, Mirocha J, Liou DZ, Leong T and Giuliano AE. Breast-conserving therapy for triple-negative breast cancer. JAMA Surg 2014; 149: 252-258.

[6] Hao NB, He YF, Li XQ, Wang K and Wang RL. The role of miRNA and LncRNA in gastric cancer. Oncotarget 2017; 8: 81572-81582.

[7] Kim D, Chang HR and Baek D. Rules for functional microRNA targeting. BMB Rep 2017; 50: 554-559.

[8] Weidle UH, Schmid D, Birzele F and Brinkmann U. MicroRNAs involved in metastasis of hepatocellular carcinoma: target candidates, functionality and efficacy in animal models and prognostic relevance. Cancer Genomics Proteomics 2020; 17: 1-21.

[9] Chen M, Li Z, Cao L, Fang C, Gao R and Liu C. miR-877-3p inhibits tumor growth and angiogenesis of osteosarcoma through fibroblast growth factor 2 signaling. Bioengineered 2022; 13: 8174-8186.

[10] Hu Y, Liang D, Chen X, Chen L, Bai J, Li H, Yin C and Zhong W. MiR-671-5p negatively regulates SMAD3 to inhibit migration and invasion of osteosarcoma cells. Nan Fang Yi Ke Da Xue Xue Bao 2021; 41: 1562-1568.

[11] Wang J, Zhang Z, Qiu C and Wang J. MicroRNA-519d-3p antagonizes osteosarcoma resistance against cisplatin by targeting PD-L1. Mol Carcinog 2022; 61: 322-333.

[12] Xue Y, Guo Y, Liu N and Meng X. MicroRNA-22-3p targeted regulating transcription factor 7-like 2 (TCF7L2) constrains the Wnt/beta-catenin pathway and malignant behavior in osteosarcoma. Bioengineered 2022; 13: 9135-9147.

[13] Zhao XG, Hu JY, Tang J, Yi W, Zhang MY, Deng R, Mai SJ, Weng NQ, Wang RQ, Liu J, Zhang HZ, He JH and Wang HY. miR-665 expression predicts poor survival and promotes tumor metastasis by targeting NR4A3 in breast cancer. Cell Death Dis 2019; 10: 479.

[14] Wang S, Du S, Lv Y, Zhang F and Wang W. MicroRNA-665 inhibits the oncogenicity of retinoblastoma by directly targeting high-mobility group box 1 and inactivating the Wnt/Beta-catenin pathway. Cancer Manag Res 2019; 11: 3111-3123.

[15] Rana R, Joon S, Chauhan K, Rathi V, Ganguly NK, Kumari C and Yadav DK. Role of extracellular vesicles in glioma progression: decipher-

ing cellular biological processes to clinical applications. Curr Top Med Chem 2021; 21: 696-704.
[16] Thery C, Ostrowski M and Segura E. Membrane vesicles as conveyors of immune responses. Nat Rev Immunol 2009; 9: 581-93.
[17] Koritzinsky EH, Street JM, Star RA and Yuen PS. Quantification of exosomes. J Cell Physiol 2017; 232: 1587-1590.
[18] Steinbichler TB, Dudas J, Riechelmann H and Skvortsova II. The role of exosomes in cancer metastasis. Semin Cancer Biol 2017; 44: 170-181.
[19] Meng F, Henson R, Wehbe-Janek H, Ghoshal K, Jacob ST and Patel T. MicroRNA-21 regulates expression of the PTEN tumor suppressor gene in human hepatocellular cancer. Gastroenterology 2007; 133: 647-658.
[20] Volinia S, Calin GA, Liu CG, Ambs S, Cimmino A, Petrocca F, Visone R, Iorio M, Roldo C, Ferracin M, Prueitt RL, Yanaihara N, Lanza G, Scarpa A, Vecchione A, Negrini M, Harris CC and Croce CM. A microRNA expression signature of human solid tumors defines cancer gene targets. Proc Natl Acad Sci U S A 2006; 103: 2257-61.
[21] Dinh TK, Fendler W, Chalubinska-Fendler J, Acharya SS, O'Leary C, Deraska PV, D'Andrea AD, Chowdhury D and Kozono D. Circulating miR-29a and miR-150 correlate with delivered dose during thoracic radiation therapy for non-small cell lung cancer. Radiat Oncol 2016; 11: 61.
[22] Alvarez-Erviti L, Seow Y, Yin H, Betts C, Lakhal S and Wood MJ. Delivery of siRNA to the mouse brain by systemic injection of targeted exosomes. Nat Biotechnol 2011; 29: 341-5.
[23] Kamerkar S, LeBleu VS, Sugimoto H, Yang S, Ruivo CF, Melo SA, Lee JJ and Kalluri R. Exosomes facilitate therapeutic targeting of oncogenic KRAS in pancreatic cancer. Nature 2017; 546: 498-503.
[24] Ritchie ME, Phipson B, Wu D, Hu Y, Law CW, Shi W and Smyth GK. limma powers differential expression analyses for RNA-sequencing and microarray studies. Nucleic Acids Res 2015; 43: e47.
[25] Chen H and Boutros PC. VennDiagram: a package for the generation of highly-customizable venn and euler diagrams in R. BMC Bioinformatics 2011; 12: 35.
[26] Shaikh AB, Li F, Li M, He B, He X, Chen G, Guo B, Li D, Jiang F, Dang L, Zheng S, Liang C, Liu J, Lu C, Liu B, Lu J, Wang L, Lu A and Zhang G. Present advances and future perspectives of molecular targeted therapy for osteosarcoma. Int J Mol Sci 2016; 17: 506.
[27] Meltzer PS and Helman LJ. New horizons in the treatment of osteosarcoma. N Engl J Med 2021; 385: 2066-2076.
[28] McEachron TA and Helman LJ. Recent advances in pediatric cancer research. Cancer Res 2021; 81: 5783-5799.
[29] Zhang K, Dong C, Chen M, Yang T, Wang X, Gao Y, Wang L, Wen Y, Chen G, Wang X, Yu X, Zhang Y, Wang P, Shang M, Han K and Zhou Y. Extracellular vesicle-mediated delivery of miR-101 inhibits lung metastasis in osteosarcoma. Theranostics 2020; 10: 411-425.
[30] Zhu KP, Zhang CL, Ma XL, Hu JP, Cai T and Zhang L. Analyzing the interactions of mRNAs and ncRNAs to predict competing endogenous RNA networks in osteosarcoma chemo-resistance. Mol Ther 2019; 27: 518-530.
[31] Fevrier B and Raposo G. Exosomes: endosomal-derived vesicles shipping extracellular messages. Curr Opin Cell Biol 2004; 16: 415-21.
[32] Wang Y, Li M, Chen L, Bian H, Chen X, Zheng H, Yang P, Chen Q and Xu H. Natural killer cell-derived exosomal miR-1249-3p attenuates insulin resistance and inflammation in mouse models of type 2 diabetes. Signal Transduct Target Ther 2021; 6: 409.
[33] Cai H, Yang X, Gao Y, Xu Z, Yu B, Xu T, Li X, Xu W, Wang X and Hua L. Exosomal microRNA-9-3p secreted from BMSCs downregulates ESM1 to suppress the development of bladder cancer. Mol Ther Nucleic Acids 2019; 18: 787-800.
[34] Basu B and Ghosh MK. Extracellular vesicles in glioma: from diagnosis to therapy. Bioessays 2019; 41: e1800245.
[35] Thery C, Amigorena S, Raposo G and Clayton A. Isolation and characterization of exosomes from cell culture supernatants and biological fluids. Curr Protoc Cell Biol 2006; Chapter 3: Unit 3.22.
[36] Wahlgren J, De L Karlson T, Brisslert M, Vaziri Sani F, Telemo E, Sunnerhagen P and Valadi H. Plasma exosomes can deliver exogenous short interfering RNA to monocytes and lymphocytes. Nucleic Acids Res 2012; 40: e130.
[37] Raimondi L, De Luca A, Gallo A, Costa V, Russelli G, Cuscino N, Manno M, Raccosta S, Carina V, Bellavia D, Conigliaro A, Alessandro R, Fini M, Conaldi PG and Giavaresi G. Osteosarcoma cell-derived exosomes affect tumor microenvironment by specific packaging of microRNAs. Carcinogenesis 2020; 41: 666-677.
[38] Gong L, Bao Q, Hu C, Wang J, Zhou Q, Wei L, Tong L, Zhang W and Shen Y. Exosomal miR-675 from metastatic osteosarcoma promotes cell migration and invasion by targeting CALN1. Biochem Biophys Res Commun 2018; 500: 170-176.
[39] Shimbo K, Miyaki S, Ishitobi H, Kato Y, Kubo T, Shimose S and Ochi M. Exosome-formed synthetic microRNA-143 is transferred to osteosarcoma cells and inhibits their migration. Biochem Biophys Res Commun 2014; 445: 381-7.

[40] Wang Z, Lin M, He L, Qi H, Shen J and Ying K. Exosomal lncRNA SCIRT/miR-665 transferring promotes lung cancer cell metastasis through the inhibition of HEYL. J Oncol 2021; 2021: 9813773.

[41] Zhou P, Xiong T, Yao L and Yuan J. MicroRNA-665 promotes the proliferation of ovarian cancer cells by targeting SRCIN1. Exp Ther Med 2020; 19: 1112-1120.

[42] Dong C, Du Q, Wang Z, Wang Y, Wu S and Wang A. MicroRNA-665 suppressed the invasion and metastasis of osteosarcoma by directly inhibiting RAB23. Am J Transl Res 2016; 8: 4975-4981.